SN 1987A: A LINEAR POLARIMETRIC STUDY

M. MÉNDEZ,[1] A. CLOCCHIATTI,[1] O. G. BENVENUTO,[2] C. FEINSTEIN,[1] AND H. G. MARRACO[3]

Facultad de Ciencias Astronómicas y Geofísicas, Universidad Nacional de La Plata

ABSTRACT

Multicolor linear polarimetric observations of SN 1987A obtained from 1987 February 28 until 1987 April 29 are presented. A correction for foreground interstellar polarization is performed, and an instrinsic polarization (IP) is obtained. The IP was decreasing at a constant position angle of 27° during the first month after the explosion. The wavelength dependence suggests that this polarization was due to Thomson scattering. However, 30 days after the explosion the polarization began to grow in the V, R, and I filters, at a different position angle, changing the wavelength dependence.

In order to interpret the behavior of the IP during the first month a model is proposed. The expansion of the outer layers of the supernova and the evolution of the photospheric density are computed. An estimation of the mass of this expanding shell is also obtained.

Subject headings: polarization — stars: individual (SN 1987A) — stars: supernovae

I. INTRODUCTION

On 1987 February 23 a supernova explosion occurred in the LMC, giving an exceptional opportunity for studying such events in a neighbor galaxy. The high apparent brightness reached by this object made it possible to obtain good quality observations, even using small telescopes, such as the one which produced the bulk of the measurements used in this work. Although extensive amounts of data related to supernova events existed at the time of the explosion of SN 1987A, little information was available concerning their polarimetric properties (see Shapiro and Sutherland 1982, for a review). Observations of linear polarization of SN 1987A have been obtained beginning on 1987 February 25 (Cropper and Bailey 1987), and from the very early moments it was seen that the polarization was variable with time. Initially, the trend of the observed polarization was decreasing (Benvenuto et al. 1987), while the observed variations were large enough to be recognized as real. Since the polarization produced by the interstellar matter is time independent, it follows that an intrinsic polarization vector (IP) should be responsible for the time-dependent characteristic. Also, the wavelength dependence of the observed polarization was far from the well-known interstellar relation (Serkowski, Mathewson, and Ford 1975), supporting the previous conclusion. In addition, as the time scale of the changes of the polarization was in the order of days, it was natural to relate them with the expansion of the external regions of the supernova.

The sole fact of the existence of an IP poses interesting problems that should be solved. One of them is the problem of correctly separating the observed polarization in a foreground polarization, produced by the aligned interstellar matter located between us and SN 1987A, and the actual IP. This is a nontrivial point. Although the wavelength dependence of the IP vector will not greatly change when using any acceptable foreground interstellar polarization (Clayton, Martin, and

Thompson 1983), its temporal behavior will be critically affected by this choice. It may be shown that the decrease detected in the observed polarization can be explained either by an increasing or decreasing IP, depending on the adopted foreground correction.

Another problem is related to the physical mechanism responsible for the polarization of the SN 1987A light. It is ordinarily accepted that the opacity of a supernova atmosphere is scattering dominated, although some absorption must be present in order to thermalize the continuum. The study of the wavelength dependence of SN 1987A polarization and its evolution with time may be helpful in testing the possible preminence of scattering over absorption. In addition, while the properties of an old supernova expanding shell will be mainly determined by its interaction with the local interstellar medium, its early behavior will be governed by the explosion itself. Thus, a model matching the polarimetric observations during the first weeks could be very useful in understanding the details of the initial expansion.

Finally, it should also be remarked that some departure from spherical symmetry must be present in order to produce a net polarization. The evolution of supernovae, as well as their using as cosmological distance indicators, may be influenced by the existence of this asymmetry. Thus, any quantitative information about its amount would be very valuable.

This paper aims at giving some insight into the problems mentioned above. In § II we present the observational data and describe the steps performed in computing the foreground polarization. In § III, a description of the IP found is given, and its possible interpretation is discussed. In § IV a model for explaining the IP is developed, and, finally, the conclusions are presented in § V.

II. OBSERVATIONS AND FOREGROUND CORRECTION

a) Observations from La Plata

The polarization measurements were carried out with the 0.83 m telescope and the rotating half-wave plate photopolarimeter of La Plata Observatory, spanning from 1987 February 28 to April 29. Standard filters B, V, R, and I of the Cousins system (Cousins 1976) were used. The instrumental polarization was determined by measuring nonpolarized

[1] On a Fellowship from CONICET.

[2] On a Fellowship from Comisión de Investigaciones Científicas de la Provincia de Buenos Aires.

[3] Member of the Carrera del Investigador Científico of CONICET, Visiting Astronomer, CASLEO, operated under agreement between the CONICET and the National Universities of La Plata, Córdoba, and San Juan.

TABLE 1

RESULTS FROM LA PLATA

DATE	FILTER	OBSERVED PARAMETERS		INTRINSIC PARAMETERS	
		$Q(\%)$	$U(\%)$	$Q(\%)$	$U(\%)$
Feb 28	B	$+0.49 \pm 0.09$	$+0.99 \pm 0.10$	$+0.48 \pm 0.09$	$+0.54 \pm 0.10$
Feb 28	V	$+0.26 \pm 0.04$	$+0.89 \pm 0.04$	$+0.25 \pm 0.04$	$+0.39 \pm 0.04$
Feb 28	R	$+0.24 \pm 0.04$	$+0.90 \pm 0.04$	$+0.23 \pm 0.04$	$+0.40 \pm 0.04$
Feb 28	I	$+0.36 \pm 0.06$	$+0.67 \pm 0.08$	$+0.35 \pm 0.06$	$+0.22 \pm 0.08$
Mar 1	B	$+0.37 \pm 0.05$	$+0.86 \pm 0.06$	$+0.36 \pm 0.05$	$+0.41 \pm 0.06$
Mar 1	V	$+0.35 \pm 0.05$	$+0.91 \pm 0.04$	$+0.34 \pm 0.05$	$+0.41 \pm 0.04$
Mar 1	R	$+0.22 \pm 0.04$	$+0.86 \pm 0.04$	$+0.21 \pm 0.04$	$+0.36 \pm 0.04$
Mar 1	I	$+0.24 \pm 0.10$	$+0.80 \pm 0.10$	$+0.23 \pm 0.10$	$+0.35 \pm 0.10$
Mar 2	B	$+0.11 \pm 0.08$	$+0.82 \pm 0.05$	$+0.10 \pm 0.08$	$+0.37 \pm 0.05$
Mar 2	V	$+0.16 \pm 0.06$	$+0.79 \pm 0.04$	$+0.15 \pm 0.06$	$+0.29 \pm 0.04$
Mar 2	R	$+0.20 \pm 0.04$	$+0.78 \pm 0.05$	$+0.19 \pm 0.04$	$+0.28 \pm 0.05$
Mar 2	I	$+0.16 \pm 0.04$	$+0.77 \pm 0.04$	$+0.15 \pm 0.04$	$+0.32 \pm 0.04$
Mar 4	B	$+0.27 \pm 0.05$	$+0.73 \pm 0.04$	$+0.26 \pm 0.05$	$+0.28 \pm 0.04$
Mar 4	V	$+0.32 \pm 0.04$	$+0.83 \pm 0.04$	$+0.31 \pm 0.04$	$+0.33 \pm 0.04$
Mar 4	R	$+0.27 \pm 0.04$	$+0.70 \pm 0.04$	$+0.26 \pm 0.04$	$+0.20 \pm 0.04$
Mar 4	I	$+0.25 \pm 0.05$	$+0.70 \pm 0.04$	$+0.24 \pm 0.05$	$+0.25 \pm 0.04$
Mar 5	B	$+0.24 \pm 0.05$	$+0.75 \pm 0.05$	$+0.23 \pm 0.05$	$+0.30 \pm 0.05$
Mar 5	V	$+0.21 \pm 0.04$	$+0.78 \pm 0.04$	$+0.20 \pm 0.04$	$+0.28 \pm 0.04$
Mar 5	R	$+0.30 \pm 0.04$	$+0.77 \pm 0.04$	$+0.29 \pm 0.04$	$+0.27 \pm 0.04$
Mar 5	I	$+0.21 \pm 0.04$	$+0.63 \pm 0.04$	$+0.20 \pm 0.04$	$+0.18 \pm 0.04$
Mar 9	V	$+0.02 \pm 0.07$	$+0.69 \pm 0.06$	$+0.01 \pm 0.07$	$+0.19 \pm 0.06$
Mar 9	R	$+0.26 \pm 0.09$	$+0.65 \pm 0.04$	$+0.25 \pm 0.09$	$+0.15 \pm 0.04$
Mar 6	B	$+0.25 \pm 0.05$	$+0.73 \pm 0.06$	$+0.24 \pm 0.05$	$+0.28 \pm 0.06$
Mar 6	V	$+0.23 \pm 0.05$	$+0.75 \pm 0.04$	$+0.22 \pm 0.05$	$+0.25 \pm 0.04$
Mar 6	R	$+0.24 \pm 0.06$	$+0.69 \pm 0.04$	$+0.23 \pm 0.06$	$+0.19 \pm 0.04$
Mar 6	I	$+0.26 \pm 0.06$	$+0.67 \pm 0.06$	$+0.25 \pm 0.06$	$+0.22 \pm 0.06$
Mar 10	B	$+0.23 \pm 0.07$	$+0.70 \pm 0.06$	$+0.22 \pm 0.07$	$+0.25 \pm 0.06$
Mar 10	V	$+0.07 \pm 0.06$	$+0.66 \pm 0.04$	$+0.06 \pm 0.06$	$+0.16 \pm 0.04$
Mar 10	R	$+0.19 \pm 0.04$	$+0.69 \pm 0.06$	$+0.18 \pm 0.04$	$+0.19 \pm 0.06$
Mar 10	I	$+0.13 \pm 0.04$	$+0.62 \pm 0.05$	$+0.12 \pm 0.04$	$+0.17 \pm 0.05$
Mar 11	B	$+0.23 \pm 0.07$	$+0.64 \pm 0.04$	$+0.22 \pm 0.07$	$+0.19 \pm 0.04$
Mar 11	V	$+0.19 \pm 0.04$	$+0.68 \pm 0.04$	$+0.18 \pm 0.04$	$+0.18 \pm 0.04$
Mar 11	R	$+0.13 \pm 0.04$	$+0.65 \pm 0.04$	$+0.12 \pm 0.04$	$+0.15 \pm 0.04$
Mar 11	I	$+0.15 \pm 0.04$	$+0.62 \pm 0.05$	$+0.14 \pm 0.04$	$+0.17 \pm 0.05$
Mar 12	B	$+0.16 \pm 0.06$	$+0.64 \pm 0.10$	$+0.15 \pm 0.06$	$+0.19 \pm 0.10$
Mar 12	V	$+0.22 \pm 0.05$	$+0.73 \pm 0.04$	$+0.21 \pm 0.05$	$+0.23 \pm 0.04$
Mar 12	R	$+0.14 \pm 0.05$	$+0.70 \pm 0.04$	$+0.13 \pm 0.05$	$+0.20 \pm 0.04$
Mar 12	I	$+0.20 \pm 0.05$	$+0.64 \pm 0.05$	$+0.19 \pm 0.06$	$+0.19 \pm 0.05$
Mar 13	B	$+0.05 \pm 0.05$	$+0.62 \pm 0.06$	$+0.04 \pm 0.05$	$+0.17 \pm 0.06$
Mar 13	V	$+0.13 \pm 0.04$	$+0.63 \pm 0.04$	$+0.12 \pm 0.04$	$+0.13 \pm 0.04$
Mar 13	R	$+0.16 \pm 0.04$	$+0.58 \pm 0.04$	$+0.15 \pm 0.04$	$+0.08 \pm 0.04$
Mar 13	I	$+0.02 \pm 0.04$	$+0.55 \pm 0.04$	$+0.01 \pm 0.04$	$+0.10 \pm 0.04$
Mar 15	B	$+0.03 \pm 0.07$	$+0.56 \pm 0.06$	$+0.02 \pm 0.07$	$+0.11 \pm 0.06$
Mar 15	V	$+0.09 \pm 0.07$	$+0.60 \pm 0.06$	$+0.08 \pm 0.07$	$+0.10 \pm 0.06$
Mar 15	R	$+0.11 \pm 0.04$	$+0.59 \pm 0.04$	$+0.10 \pm 0.04$	$+0.09 \pm 0.04$
Mar 15	I	$+0.13 \pm 0.04$	$+0.53 \pm 0.04$	$+0.12 \pm 0.04$	$+0.08 \pm 0.04$
Mar 16	B	$+0.14 \pm 0.04$	$+0.73 \pm 0.06$	$+0.13 \pm 0.04$	$+0.28 \pm 0.06$
Mar 16	V	$+0.08 \pm 0.04$	$+0.58 \pm 0.04$	$+0.07 \pm 0.04$	$+0.08 \pm 0.04$
Mar 16	R	$+0.13 \pm 0.05$	$+0.57 \pm 0.05$	$+0.12 \pm 0.05$	$+0.07 \pm 0.05$
Mar 16	I	$+0.18 \pm 0.05$	$+0.58 \pm 0.05$	$+0.17 \pm 0.05$	$+0.13 \pm 0.05$
Mar 17	B	$+0.24 \pm 0.07$	$+0.94 \pm 0.07$	$+0.23 \pm 0.07$	$+0.49 \pm 0.07$
Mar 17	V	$+0.16 \pm 0.04$	$+0.66 \pm 0.04$	$+0.15 \pm 0.04$	$+0.16 \pm 0.04$
Mar 17	R	$+0.22 \pm 0.05$	$+0.63 \pm 0.04$	$+0.21 \pm 0.05$	$+0.13 \pm 0.04$
Mar 17	I	$+0.28 \pm 0.04$	$+0.76 \pm 0.06$	$+0.27 \pm 0.04$	$+0.31 \pm 0.06$
Mar 22	B	$+0.00 \pm 0.06$	$+0.50 \pm 0.07$	-0.01 ± 0.06	$+0.05 \pm 0.07$
Mar 22	V	-0.01 ± 0.04	$+0.52 \pm 0.05$	-0.02 ± 0.04	$+0.02 \pm 0.05$
Mar 22	R	$+0.15 \pm 0.08$	$+0.52 \pm 0.04$	$+0.14 \pm 0.08$	$+0.02 \pm 0.04$
Mar 22	I	$+0.09 \pm 0.11$	$+0.37 \pm 0.04$	$+0.08 \pm 0.11$	-0.08 ± 0.04
Mar 25	B	-0.07 ± 0.05	$+0.39 \pm 0.04$	-0.08 ± 0.05	-0.06 ± 0.04
Mar 25	V	$+0.00 \pm 0.04$	$+0.32 \pm 0.04$	-0.01 ± 0.04	-0.18 ± 0.04
Mar 25	R	$+0.02 \pm 0.04$	$+0.41 \pm 0.04$	$+0.01 \pm 0.04$	-0.09 ± 0.04
Mar 25	I	-0.07 ± 0.04	$+0.39 \pm 0.04$	-0.08 ± 0.04	-0.06 ± 0.04
Mar 26	B	$+0.01 \pm 0.06$	$+0.63 \pm 0.05$	$+0.00 \pm 0.06$	$+0.18 \pm 0.05$
Mar 26	V	$+0.10 \pm 0.04$	$+0.51 \pm 0.05$	$+0.09 \pm 0.04$	$+0.01 \pm 0.05$
Mar 26	R	$+0.08 \pm 0.04$	$+0.53 \pm 0.04$	$+0.07 \pm 0.04$	$+0.03 \pm 0.04$
Mar 26	I	$+0.09 \pm 0.04$	$+0.34 \pm 0.06$	$+0.08 \pm 0.04$	-0.11 ± 0.06
Mar 27	B	$+0.12 \pm 0.04$	$+0.64 \pm 0.09$	$+0.11 \pm 0.04$	$+0.19 \pm 0.09$
Mar 27	V	$+0.09 \pm 0.05$	$+0.48 \pm 0.04$	$+0.08 \pm 0.05$	-0.02 ± 0.04
Mar 27	R	$+0.21 \pm 0.04$	$+0.42 \pm 0.05$	$+0.20 \pm 0.04$	-0.08 ± 0.05

296

TABLE 1—*Continued*

DATE	FILTER	OBSERVED PARAMETERS		INTRINSIC PARAMETERS	
		$Q(\%)$	$U(\%)$	$Q(\%)$	$U(\%)$
Mar 27	I	$+0.20 \pm 0.04$	$+0.27 \pm 0.06$	$+0.19 \pm 0.04$	-0.18 ± 0.06
Apr 1	B	-0.01 ± 0.05	$+0.67 \pm 0.06$	-0.02 ± 0.05	$+0.22 \pm 0.06$
Apr 1	V	$+0.02 \pm 0.04$	$+0.42 \pm 0.04$	$+0.01 \pm 0.04$	-0.08 ± 0.04
Apr 1	R	$+0.12 \pm 0.04$	$+0.38 \pm 0.05$	$+0.11 \pm 0.04$	-0.12 ± 0.05
Apr 1	I	$+0.16 \pm 0.04$	$+0.20 \pm 0.04$	$+0.15 \pm 0.04$	-0.25 ± 0.04
Apr 6	V	$+0.18 \pm 0.04$	$+0.58 \pm 0.04$	$+0.17 \pm 0.04$	$+0.08 \pm 0.04$
Apr 8	B	$+0.09 \pm 0.06$	$+0.75 \pm 0.04$	$+0.08 \pm 0.06$	$+0.30 \pm 0.04$
Apr 8	V	$+0.26 \pm 0.04$	$+0.56 \pm 0.04$	$+0.25 \pm 0.04$	$+0.06 \pm 0.04$
Apr 8	R	$+0.32 \pm 0.04$	$+0.48 \pm 0.04$	$+0.31 \pm 0.04$	-0.02 ± 0.04
Apr 8	I	$+0.17 \pm 0.04$	$+0.39 \pm 0.04$	$+0.16 \pm 0.04$	-0.06 ± 0.04
Apr 9	B	$+0.08 \pm 0.04$	$+0.59 \pm 0.04$	$+0.07 \pm 0.04$	$+0.14 \pm 0.04$
Apr 9	V	$+0.21 \pm 0.04$	$+0.57 \pm 0.04$	$+0.20 \pm 0.04$	$+0.07 \pm 0.04$
Apr 9	I	$+0.09 \pm 0.04$	$+0.36 \pm 0.04$	$+0.08 \pm 0.04$	-0.09 ± 0.04
Apr 10	B	$+0.07 \pm 0.06$	$+0.71 \pm 0.04$	$+0.06 \pm 0.06$	$+0.26 \pm 0.04$
Apr 10	V	$+0.10 \pm 0.04$	$+0.57 \pm 0.04$	$+0.09 \pm 0.04$	$+0.07 \pm 0.04$
Apr 10	R	$+0.13 \pm 0.05$	$+0.47 \pm 0.04$	$+0.12 \pm 0.05$	-0.03 ± 0.04
Apr 10	I	$+0.05 \pm 0.04$	$+0.33 \pm 0.04$	$+0.04 \pm 0.04$	-0.12 ± 0.04
Apr 12	B	$+0.27 \pm 0.06$	$+0.77 \pm 0.04$	$+0.26 \pm 0.06$	$+0.32 \pm 0.04$
Apr 12	V	$+0.26 \pm 0.04$	$+0.47 \pm 0.04$	$+0.25 \pm 0.04$	-0.03 ± 0.04
Apr 12	R	$+0.25 \pm 0.04$	$+0.41 \pm 0.05$	$+0.24 \pm 0.04$	-0.09 ± 0.05
Apr 12	I	$+0.17 \pm 0.04$	$+0.28 \pm 0.04$	$+0.16 \pm 0.04$	-0.17 ± 0.04
Apr 17	B	$+0.12 \pm 0.05$	$+0.64 \pm 0.05$	$+0.11 \pm 0.05$	$+0.19 \pm 0.05$
Apr 17	V	$+0.26 \pm 0.04$	$+0.58 \pm 0.04$	$+0.25 \pm 0.04$	$+0.08 \pm 0.04$
Apr 17	R	$+0.21 \pm 0.10$	$+0.45 \pm 0.05$	$+0.20 \pm 0.10$	-0.05 ± 0.05
Apr 17	I	$+0.25 \pm 0.05$	$+0.38 \pm 0.04$	$+0.24 \pm 0.05$	-0.07 ± 0.04
Apr 23	B	$+0.06 \pm 0.05$	$+0.61 \pm 0.05$	$+0.05 \pm 0.05$	$+0.16 \pm 0.05$
Apr 23	V	$+0.19 \pm 0.04$	$+0.52 \pm 0.04$	$+0.18 \pm 0.04$	$+0.02 \pm 0.04$
Apr 23	I	$+0.24 \pm 0.05$	$+0.24 \pm 0.04$	$+0.23 \pm 0.05$	-0.21 ± 0.04
Apr 29	B	$+0.18 \pm 0.04$	$+0.63 \pm 0.04$	$+0.17 \pm 0.04$	$+0.18 \pm 0.04$
Apr 29	V	$+0.23 \pm 0.04$	$+0.49 \pm 0.04$	$+0.22 \pm 0.04$	-0.01 ± 0.04

nearby stars, selected from the *Catalogue of Nearby Stars* (Gliese 1969), and, finally, the observations were reduced to the standard equatorial system by using highly polarized stars from the list of Serkowski, Mathewson, and Ford (1975). Repeated observations of these standard stars were made in all filters during each night in order to check the stability of the system. It was found unnecessary to correct for depolarization. The observational error was monitored in real time during the observation, and data gathering was interrupted when the desired error level (0.03% in the polarization) was attained. Typical integration times were 300 s for the *B* filter, 90 s for the *V* filter, and 45 s for *R* and *I* filters. The observational data are summarized in Table 1.

b) Observations from San Juan

The 2.15 m telescope of the Complejo Astronómico " El Leoncito" (CASLEO), together with the Vatican Observatory Polarimeter (VATPOL), which is described by Magalhaes, Benedetti, and Roland (1984), were employed. *UBVRI* measurements from the supernova were obtained from 1987 April 2 to April 10. In order to determine the foreground interstellar polarization, observations of the LMC star Sk −69°203 (Sanduleak 1970) were performed. The corrections for the instrumental effects were carried out in a similar way, as mentioned above. The data are shown in Table 2.

In both cases the observations were corrected for sky polarization by measuring different star-free zones around the object studied.

c) Observations from the Literature

Since we could not observe the SN 1987A before 1987 February 28, some linear polarimetric observations were selected from the IAU circulars in order to cover its behavior during the first few days after the explosion and to improve the later analysis. The selected observations are shown in Table 3.

d) Foreground Correction

As mentioned above, a LMC star near the SN field was observed in order to obtain the intrinsic polarization of SN 1987A, although no multicolor measurements could be done in this case. The correction was estimated as follows. Following Clayton, Martin, and Thompson (1983), the measured polarization for Sk −69°203 was taken to be P_{max} for the foreground material, while normal values of λ_{max} and k were assumed following the relation $k = 1.84 \lambda_{max} - 0.10$ (Wilking, Lebofsky, and Rieke 1982). Then $P(\lambda)$ was calculated for each passband using the Serkowski interstellar relation. The corresponding Stokes parameters were computed and subtracted from those of SN 1987A to achieve its intrinsic polarization. The same correction was applied to all of the observations, including those coming from the IAU circulars.

It might be argued that using a single interstellar $P(\lambda)$ curve to correct for the combined effects of the Galaxy and LMC could be quite rough. However, it may be justified as follows. According to previous studies in the LMC region (Schmidt 1976; Clayton, Martin, and Thompson 1983), the interstellar polarization of both the Galaxy and LMC behave normally. We have extensively tested the superposition of two Serkowski interstellar curves of arbitrary orientations, with parameters in the range of those observed by the named authors, and we have obtained $P(\lambda)$ versus λ curves which, in all cases, display a similar interstellar behavior. Thus, having in mind the large errors involved in estimating foreground polarizations, the use of a single correction appears to be reasonable. Moreover, this

TABLE 2

RESULTS FROM SAN JUAN

DATE	FILTER	OBSERVED PARAMETERS		INTRINSIC PARAMETERS	
		$Q(\%)$	$U(\%)$	$Q(\%)$	$U(\%)$
Apr 2	U	$+0.02 \pm 0.05$	$+0.48 \pm 0.05$	$+0.01 \pm 0.05$	$+0.09 \pm 0.05$
Apr 2	B	$+0.04 \pm 0.06$	$+0.66 \pm 0.06$	$+0.03 \pm 0.06$	$+0.21 \pm 0.06$
Apr 2	V	$+0.11 \pm 0.04$	$+0.44 \pm 0.04$	$+0.10 \pm 0.04$	-0.06 ± 0.04
Apr 2	R	$+0.20 \pm 0.05$	$+0.33 \pm 0.05$	$+0.19 \pm 0.05$	-0.17 ± 0.05
Apr 2	I	$+0.15 \pm 0.03$	$+0.29 \pm 0.03$	$+0.14 \pm 0.03$	-0.16 ± 0.03
Apr 3	U	-0.05 ± 0.03	$+0.49 \pm 0.03$	-0.06 ± 0.03	$+0.10 \pm 0.03$
Apr 3	B	-0.06 ± 0.05	$+0.62 \pm 0.05$	-0.07 ± 0.05	$+0.17 \pm 0.05$
Apr 3	V	$+0.07 \pm 0.03$	$+0.45 \pm 0.03$	$+0.06 \pm 0.03$	-0.05 ± 0.03
Apr 3	R	$+0.21 \pm 0.04$	$+0.36 \pm 0.04$	$+0.20 \pm 0.04$	-0.14 ± 0.04
Apr 3	I	$+0.15 \pm 0.02$	$+0.31 \pm 0.02$	$+0.14 \pm 0.02$	-0.14 ± 0.02
Apr 4	U	$+0.07 \pm 0.03$	$+0.38 \pm 0.03$	$+0.06 \pm 0.03$	-0.01 ± 0.03
Apr 4	B	$+0.05 \pm 0.04$	$+0.52 \pm 0.04$	$+0.04 \pm 0.04$	$+0.07 \pm 0.04$
Apr 4	V	$+0.14 \pm 0.04$	$+0.44 \pm 0.04$	$+0.13 \pm 0.04$	-0.06 ± 0.04
Apr 4	R	$+0.23 \pm 0.03$	$+0.34 \pm 0.03$	$+0.22 \pm 0.03$	-0.16 ± 0.03
Apr 4	I	$+0.16 \pm 0.03$	$+0.28 \pm 0.03$	$+0.15 \pm 0.03$	-0.17 ± 0.03
Apr 5	U	$+0.00 \pm 0.02$	$+0.46 \pm 0.02$	-0.01 ± 0.02	$+0.07 \pm 0.02$
Apr 5	B	-0.05 ± 0.03	$+0.56 \pm 0.03$	-0.06 ± 0.03	$+0.11 \pm 0.03$
Apr 5	V	$+0.11 \pm 0.02$	$+0.42 \pm 0.02$	$+0.10 \pm 0.02$	-0.08 ± 0.02
Apr 5	R	$+0.21 \pm 0.02$	$+0.36 \pm 0.02$	$+0.20 \pm 0.02$	-0.14 ± 0.02
Apr 5	I	$+0.19 \pm 0.02$	$+0.27 \pm 0.02$	$+0.18 \pm 0.02$	-0.18 ± 0.02
Apr 6	U	$+0.08 \pm 0.04$	$+0.45 \pm 0.04$	$+0.07 \pm 0.04$	$+0.06 \pm 0.04$
Apr 6	B	$+0.08 \pm 0.05$	$+0.57 \pm 0.05$	$+0.07 \pm 0.05$	$+0.12 \pm 0.05$
Apr 6	V	$+0.07 \pm 0.05$	$+0.42 \pm 0.05$	$+0.06 \pm 0.05$	-0.08 ± 0.05
Apr 6	R	$+0.22 \pm 0.02$	$+0.38 \pm 0.02$	$+0.21 \pm 0.02$	-0.12 ± 0.02
Apr 6	I	$+0.26 \pm 0.04$	$+0.31 \pm 0.04$	$+0.25 \pm 0.04$	-0.14 ± 0.04
Apr 7	U	-0.01 ± 0.04	$+0.48 \pm 0.04$	-0.02 ± 0.04	$+0.09 \pm 0.04$
Apr 7	B	$+0.13 \pm 0.03$	$+0.54 \pm 0.03$	$+0.12 \pm 0.03$	$+0.09 \pm 0.03$
Apr 7	V	$+0.11 \pm 0.03$	$+0.47 \pm 0.03$	$+0.10 \pm 0.03$	-0.03 ± 0.03
Apr 7	R	$+0.25 \pm 0.03$	$+0.32 \pm 0.03$	$+0.24 \pm 0.03$	-0.18 ± 0.03
Apr 7	I	$+0.22 \pm 0.03$	$+0.30 \pm 0.03$	$+0.21 \pm 0.03$	-0.15 ± 0.03
Apr 8	U	$+0.06 \pm 0.03$	$+0.53 \pm 0.03$	$+0.05 \pm 0.03$	$+0.14 \pm 0.03$
Apr 8	B	$+0.11 \pm 0.04$	$+0.61 \pm 0.04$	$+0.10 \pm 0.04$	$+0.16 \pm 0.04$
Apr 8	V	$+0.12 \pm 0.02$	$+0.48 \pm 0.02$	$+0.11 \pm 0.02$	-0.02 ± 0.02
Apr 8	R	$+0.23 \pm 0.03$	$+0.36 \pm 0.03$	$+0.22 \pm 0.03$	-0.14 ± 0.03
Apr 8	I	$+0.24 \pm 0.03$	$+0.32 \pm 0.03$	$+0.23 \pm 0.03$	-0.13 ± 0.03
Apr 9	U	$+0.05 \pm 0.03$	$+0.52 \pm 0.03$	$+0.04 \pm 0.03$	$+0.13 \pm 0.03$
Apr 9	B	$+0.06 \pm 0.03$	$+0.60 \pm 0.03$	$+0.05 \pm 0.03$	$+0.15 \pm 0.03$
Apr 9	V	$+0.20 \pm 0.03$	$+0.47 \pm 0.03$	$+0.19 \pm 0.03$	-0.03 ± 0.03
Apr 9	R	$+0.34 \pm 0.03$	$+0.40 \pm 0.03$	$+0.33 \pm 0.03$	-0.10 ± 0.03
Apr 9	I	$+0.27 \pm 0.04$	$+0.31 \pm 0.04$	$+0.26 \pm 0.04$	-0.14 ± 0.04
Apr 10	U	$+0.08 \pm 0.04$	$+0.56 \pm 0.04$	$+0.07 \pm 0.04$	$+0.17 \pm 0.04$
Apr 10	B	$+0.15 \pm 0.04$	$+0.65 \pm 0.04$	$+0.14 \pm 0.04$	$+0.20 \pm 0.04$
Apr 10	V	$+0.19 \pm 0.02$	$+0.49 \pm 0.02$	$+0.18 \pm 0.02$	-0.01 ± 0.02
Apr 10	R	$+0.27 \pm 0.03$	$+0.37 \pm 0.03$	$+0.26 \pm 0.03$	-0.13 ± 0.03
Apr 10	I	$+0.25 \pm 0.02$	$+0.31 \pm 0.02$	$+0.24 \pm 0.02$	-0.14 ± 0.02

correction will not alter significantly the wavelength dependence of either its intrinsic polarization or its orientation (Clayton, Martin, and Thompson 1983). The observed linear polarization of Sk $-69°203$, in the passband defined by the RCA 31034 A photomultiplier and the optical system, is $p = 0.50\%$ at an angle of $44°$. This value is similar to that obtained by Schmidt (1976) for the field of SN 1987A in his study of the foreground polarization of the Milky Way in the Magellanic Cloud Region. This result suggests that, in the region under study, the contribution of the LMC interstellar material to the total foreground polarization is low, strengthening the hypothesis of a single $P(\lambda)$ curve. The foreground polarization used is summarized in Table 4.

III. THE INTRINSIC POLARIZATION

When the foreground interstellar polarization vector is subtracted from all measurements, the results presented in Tables 1, 2, 3 and Figure 1 are obtained. There are some features that

should be remarked. First, after removing foreground polarization, there still remains an intrinsic component (IP), which is greater than the errors involved, and whose wavelength dependence is clearly not interstellar. Second, the behavior of the IP is similar in all wavelengths during the first 4 weeks after explosion. Third, neglecting irregular variations probably due to some random characteristic of the expansion produced by the explosion, the IP shows a decreasing trend with time, at a position angle of $\sim 27°$ which is both wavelength and time independent. This result differs from that obtained by Schwarz and Mundt (1987), as they found an IP vector growing with time. However, the difference is due to the foreground correction applied in each case. When their *UBVRI* observations are corrected with our foreground polarization (we have indeed used them in this work), they display the same trend as the others. The correction used by these authors was obtained from a star of magnitude $V = 10.3$ (Barret 1987a), which almost certainly belongs to the Galaxy. The observed polariz-

TABLE 3

RESULTS FROM THE LITERATURE

DATE	FILTER	OBSERVED PARAMETERS		INTRINSIC PARAMETERS		SOURCE
		$Q(\%)$	$U(\%)$	$Q(\%)$	$U(\%)$	
Feb 25	U	$+0.38 \pm 0.10$	$+0.94 \pm 0.10$	$+0.37 \pm 0.10$	$+0.55 \pm 0.10$	1
Feb 25	B	$+0.30 \pm 0.06$	$+0.92 \pm 0.06$	$+0.29 \pm 0.06$	$+0.47 \pm 0.06$	1
Feb 25	V	-0.03 ± 0.08	$+0.83 \pm 0.08$	-0.04 ± 0.08	$+0.33 \pm 0.08$	1
Feb 25	R	$+0.03 \pm 0.06$	$+0.86 \pm 0.06$	$+0.02 \pm 0.06$	$+0.36 \pm 0.06$	1
Feb 25	I	$+0.11 \pm 0.04$	$+0.80 \pm 0.04$	$+0.10 \pm 0.04$	$+0.35 \pm 0.04$	1
Feb 28	U	$+0.19 \pm 0.22$	$+0.90 \pm 0.22$	$+0.18 \pm 0.22$	$+0.51 \pm 0.22$	2
Feb 28	B	$+0.57 \pm 0.18$	$+0.72 \pm 0.18$	$+0.56 \pm 0.18$	$+0.27 \pm 0.18$	2
Feb 28	V	$+0.17 \pm 0.09$	$+0.95 \pm 0.09$	$+0.16 \pm 0.09$	$+0.45 \pm 0.09$	2
Feb 28	R	$+0.18 \pm 0.01$	$+0.84 \pm 0.01$	$+0.17 \pm 0.01$	$+0.34 \pm 0.01$	2
Feb 28	I	$+0.21 \pm 0.03$	$+0.65 \pm 0.03$	$+0.20 \pm 0.03$	$+0.20 \pm 0.03$	2
Mar 1	V	$+0.29 \pm 0.09$	$+0.80 \pm 0.09$	$+0.28 \pm 0.09$	$+0.30 \pm 0.09$	2
Mar 2	U	$+0.31 \pm 0.11$	$+0.49 \pm 0.11$	$+0.30 \pm 0.11$	$+0.10 \pm 0.11$	2
Mar 2	B	$+0.22 \pm 0.10$	$+0.89 \pm 0.10$	$+0.21 \pm 0.10$	$+0.44 \pm 0.10$	2
Mar 2	R	$+0.19 \pm 0.08$	$+0.77 \pm 0.08$	$+0.18 \pm 0.08$	$+0.27 \pm 0.08$	2
Mar 2	I	$+0.09 \pm 0.10$	$+0.63 \pm 0.10$	$+0.08 \pm 0.10$	$+0.18 \pm 0.10$	2
Mar 6	U	-0.06 ± 0.06	$+0.58 \pm 0.06$	-0.07 ± 0.06	$+0.19 \pm 0.06$	3
Mar 6	B	$+0.22 \pm 0.06$	$+0.60 \pm 0.06$	$+0.21 \pm 0.06$	$+0.15 \pm 0.06$	3
Mar 6	V	$+0.26 \pm 0.07$	$+0.58 \pm 0.07$	$+0.25 \pm 0.07$	$+0.08 \pm 0.07$	3
Mar 6	R	$+0.19 \pm 0.05$	$+0.57 \pm 0.05$	$+0.18 \pm 0.05$	$+0.07 \pm 0.05$	3
Mar 6	I	$+0.27 \pm 0.07$	$+0.51 \pm 0.07$	$+0.26 \pm 0.07$	$+0.06 \pm 0.07$	3
Mar 7	U	$+0.11 \pm 0.12$	$+0.78 \pm 0.12$	$+0.10 \pm 0.12$	$+0.39 \pm 0.12$	4
Mar 7	B	$+0.15 \pm 0.04$	$+0.72 \pm 0.04$	$+0.14 \pm 0.04$	$+0.27 \pm 0.04$	4
Mar 7	V	$+0.21 \pm 0.07$	$+0.73 \pm 0.07$	$+0.20 \pm 0.07$	$+0.23 \pm 0.07$	4
Mar 7	R	$+0.33 \pm 0.08$	$+0.63 \pm 0.08$	$+0.32 \pm 0.08$	$+0.13 \pm 0.08$	4
Mar 7	I	$+0.21 \pm 0.07$	$+0.56 \pm 0.07$	$+0.20 \pm 0.07$	$+0.11 \pm 0.07$	4
Mar 8	U	$+0.03 \pm 0.11$	$+0.83 \pm 0.11$	$+0.02 \pm 0.11$	$+0.44 \pm 0.11$	4
Mar 8	B	$+0.13 \pm 0.05$	$+0.71 \pm 0.05$	$+0.12 \pm 0.05$	$+0.26 \pm 0.05$	4
Mar 8	V	$+0.22 \pm 0.08$	$+0.68 \pm 0.08$	$+0.21 \pm 0.08$	$+0.18 \pm 0.08$	4
Mar 8	R	$+0.23 \pm 0.09$	$+0.69 \pm 0.09$	$+0.22 \pm 0.09$	$+0.19 \pm 0.09$	4
Mar 8	I	$+0.16 \pm 0.09$	$+0.64 \pm 0.09$	$+0.15 \pm 0.09$	$+0.19 \pm 0.09$	4
Mar 21	U	-0.22 ± 0.10	$+0.46 \pm 0.10$	-0.23 ± 0.10	$+0.07 \pm 0.10$	5
Mar 21	B	$+0.17 \pm 0.07$	$+0.59 \pm 0.07$	$+0.16 \pm 0.07$	$+0.14 \pm 0.07$	5
Mar 21	V	-0.03 ± 0.07	$+0.49 \pm 0.07$	-0.04 ± 0.07	-0.01 ± 0.07	5
Mar 21	R	$+0.09 \pm 0.05$	$+0.52 \pm 0.05$	$+0.08 \pm 0.05$	$+0.02 \pm 0.05$	5
Mar 21	I	$+0.06 \pm 0.04$	$+0.44 \pm 0.04$	$+0.05 \pm 0.04$	-0.01 ± 0.04	5

SOURCES.—(1) Cropper and Bailey 1987. (2) Barret 1987a. (3) Schwarz 1987. (4) Barret 1987b.

ation for this star (0.97%) is notably different to that suggested by Schmidt (1976) for this field, which is based on the average of 13 Galactic stars. In addition, Barret (1987b) reports a variation of the polarization of this star. Thus, it seems that the star used by Schwarz and Mundt for foreground correction is intrinsically polarized, and we have preferred using our measurements of Sk −69°203.

Fourth, since 1987 March 25 approximately a change in the behavior of the IP in the VRI filters becomes notable. The initial decreasing trend is reversed, and the IP vector begins growing at a different position angle. This change is not observed in the U and B bands.

According to this last remark it seems reasonable to divide the analysis of the IP of SN 1987A in two parts: before and after March 25. The easiest way of explaining this dual behavior is allowing for the presence of two independent sources of

TABLE 4

FOREGROUND CORRECTION

Filter	λ_{eff} (μm)	$P(\%)$	$Q(\%)$	$U(\%)$
U	0.37	0.39	0.01	0.39
B	0.44	0.45	0.01	0.45
V	0.55	0.50	0.01	0.50
R	0.64	0.50	0.01	0.50
I	0.79	0.45	0.01	0.45

intrinsic polarization. One that dominates the production of polarized light in the first 4 weeks, and another that becomes important for the longer wavelengths during the second period.

The first component appears particularly clean in U and B filters, where the second component is not existent. This gives the possibility of using these colors in order to determine the direction of the evolution of the first component of the IP vector. This direction was computed by a weighted linear least squares fit (Deeming 1968), and is shown in Figures 1a–1e. In Figures 2a–2e we display the temporal behavior of the projections of the polarization parallel (Pl) and perpendicular (Pr) to this direction. During the first period Pr averages zero, while Pl displays a decreasing tendency in all filters. Moreover, the Pl projections are almost the same in all bands, suggesting a wavelength-independent polarizing mechanism. When the second component appears, this wavelength independence is lost.

According to Shapiro and Sutherland (1982), the wavelength independence of the polarization would suggest that the opacity would be purely Thomson scattering, in a medium where the ratio of the absorption to the total opacity is much less than unity. Obviously, the scattering medium will need some kind of asymmetry in order to produce a net polarization.

In this frame, it is useful the analysis of the correlation

between the total and polarized fluxes in each passband. These correlations are shown in Figures 3a–3e, where the monochromatic fluxes used were obtained from the *UBVRI* photometric observations of Hamuy *et al.* (1988), and effective wavelengths and fluxes are given by Bessell (1979). It is easy to see, from the inspection of these figures, the differences between correlations before and after 1987 March 30.

It is known that in a static scattering system where the non-polarized flux emitted is variable, the polarized and nonpolarized fluxes will be linearly correlated, and the slope of this correlation will be the polarization. Although both fluxes are variable with time, the resulting polarization, which only depends on the geometry of the system and the optical depth of the scatterers, will be time independent. On the other hand, for a nonstatic scattering system, the relation between the polarized and nonpolarized fluxes will depend on the balance of the variations of its light, optical depth, and geometry. This kind of consideration allows us to qualitatively analyze the evolution of the IP and the flux correlations presented.

The scattering expanding shell of a supernova is, clearly, a nonstatic system. However, it appears reasonable to think about this shell as evolving without greatly changing its geometry, particularly during the first period when the interaction with the local interstellar medium is negligible. The initial decreasing trend of the Pl projection can be understood as follows: The increasing nonpolarized light emitted by SN 1987A during this period is combined with a decreasing optical depth of the scattering electrons in the expanding shell. If the second process is dominant, the resulting polarized flux, as well as the polarization, will be decreasing. Concerning the second IP component, it is due to a polarized flux which is proportional to the nonpolarized one. Consequently, it should be produced in a region where the optical depth has an increasing trend. This fact, together with the disparity of the position angles, which suggests a different asymmetry, supports our previous interpretation of two different components in the polarization.

IV. THE MODEL

The observational evidence presented in the previous section can be used to set the basis for a model of the region which produced the polarization of SN 1987A. The separation of the polarization in two components of different importance during each period simplifies the analysis. The projection Pl of the first component appears as the easiest to be explained, since its wavelength independence indicates that it is produced by Thomson scattering. The existence of an intrinsic net polarization, produced by scattering, in the light of the SN 1987A necessarily implies an asymmetry in its envelope. All current models of supernova explosions are built under the assumption of spherical symmetry in order to explain the global dynamics of these events. In this frame, a small asymmetry does not appear as relevant, and it is neglected. However, it is a crucial factor in the present model. In fact, the symmetry of the actual shock is probably not spherical but axial, since it is produced in the core of a progenitor which carries a large amount of angular momentum (as it should be if protoneutron stars and pulsars are originated in this zone). Such a shock will produce an axisymmetric expanding envelope. In this frame a net polarization via Thomson scattering will be produced.

There are some theoretical approaches to the modeling of the polarization region of SN 1987A. The main question to be answered is concerned with the thickness of the scattering region. The full consideration of the radiative transfer problem
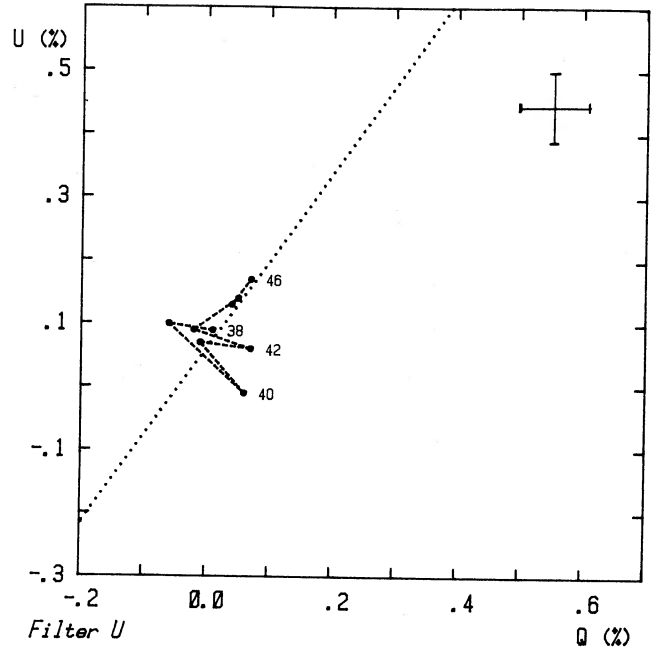
FIG. 1a
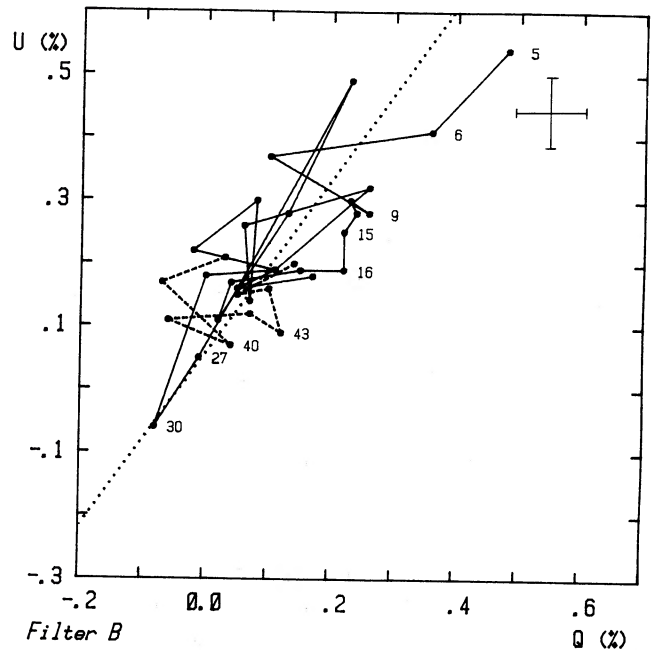
FIG. 1b

FIG. 1.—(*a*) Intrinsic polarization of SN 1987A (corrected for foreground contribution) in the *U* filter. *Dashed line*, observations from San Juan. Numbers at the right of the dots indicate days after February 23. *Dotted line*, the weighted linear least-squares fit computed using the observations in the *B* band. Representative error bar in *Q* and *U* is also indicated. (*b*) Intrinsic polarization of SN 1987A (corrected for foreground contribution) in the *B* filter. *Solid line*, observations from La Plata. *Dashed line*, observations from San Juan. Numbers and dotted line have the same meaning as in (*a*). (*c*) Same as (*b*), in the *V* filter. (*d*) Same as (*b*), in the *R* filter. (*e*) Same as (*b*), in the *I* filter.
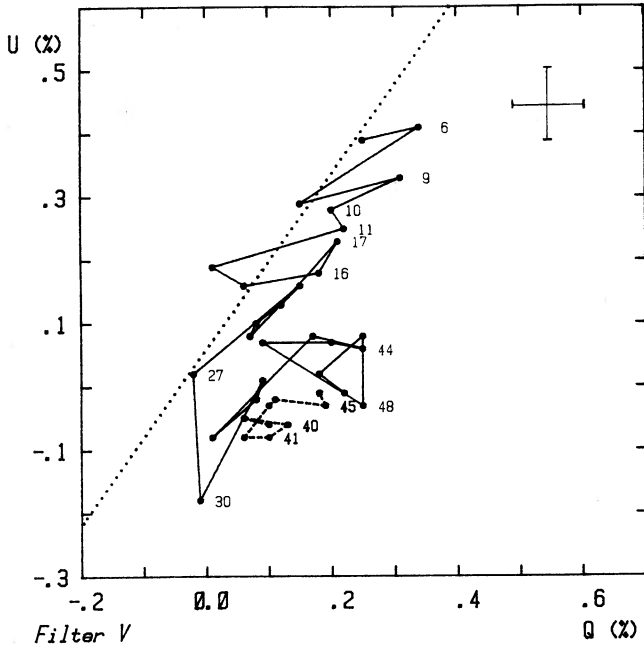
FIG. 1c
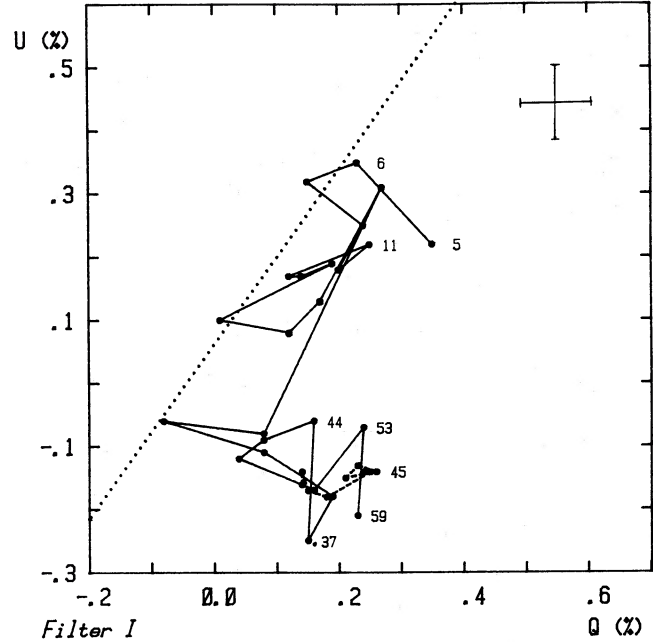
FIG. 1e
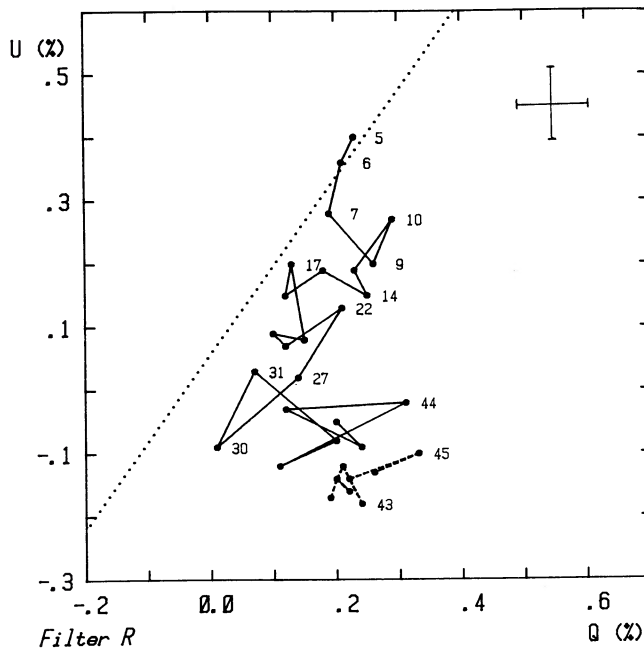
FIG. 1d

have been worked out by Shapiro and Sutherland (1982), on the assumption of a plane-parallel atmosphere. Their results provide amounts of polarization comparable with our observations. However, the temporal behavior and color dependence of the polarization of SN 1987A cannot be explained in this frame. Shapiro and Sutherland's model relates the observed net polarization with the opacity characteristics of the shell (mainly the relative importance of scattering and absorption processes), its asymmetry (measured by its asphericity or the related eccentricity), and its orientation. A change of the polarization have to be explained via changes of these parameters. Because of the constancy of the position angle of

the polarization, changes in the orientation of the shell should be rejected. Because of its observed wavelength independence, changes in the opacity must also be neglected. Finally, a substantial change of the eccentricity would be necessary to explain the observed temporal change of the polarization. As we mentioned above, such a change in the eccentricity, in a time scale of days, does not appear reasonable.

It is necessary to introduce a different theoretical frame to explain the observations. The logical following step is to introduce an extended, axisymmetric expanding atmosphere. The full consideration of the radiative transfer problem in this geometry presents such a degree of complexity that is out of the scope of the present work. In order to get some insight on the problem, we will treat the much more simple case of an optically thin envelope.

However, it is important to remark that the polarization of a scattering dominated atmosphere will be mainly produced in the optically thin regions. The polarization originated in the innermost layers will tend to be washed out by multiple scattering.

The theory of the polarization by scattering in extended, axisymmetric, optically thin envelopes was developed by Brown and McLean (1977), under the hypothesis of a point source located at the center of the envelope. Rudy (1978) showed that for the case of an extended source, a depolarizing factor must be introduced. The polarization produced by an envelope, as studied by Brown and McLean (1977), but including this depolarizing factor was given by Cassinelli, Nordsiek, and Murison (1987):

$$P = -\frac{3}{16}\sigma_T \sin^2 i \int_{r=a}^{\infty}\int_{\mu=-1}^{1}(1-3\mu^2)$$
$$\times \left(1-\frac{a^2}{r^2}\right)^{1/2}n(r,\mu)dr\,d\mu,\quad(1)$$

where $n(r,\mu)$ is the electron number density, i is the angle between the axis of symmetry of the envelope and the direction

to the observer, σ_T denotes the cross section for Thomson scattering of a single electron, μ is the cosine of the polar angle, r is the central distance in a spherical system of coordinates, and a is the radius of the illuminating source.

In order to reach further insight on the evolution of the physical parameters of the shell, an expression for $n(r, \mu)$ must be proposed. We have assumed that these shells are oblate ellipsoids of eccentricity e, and an exponential radial dependence:

$$n(r, \mu) = n_0 \exp\left[-\frac{r-a}{\xi}(1 - e^2 + e^2\mu^2)^{1/2} \right], \quad (2)$$

where n_0 is the electron number density in the photosphere, a is the radius of the photosphere, and ξ is the characteristic size of the shell. This assumption should be considered as an interpolatory approximation. The resulting expression for the polarization produced by this mass distribution may be written as the sum of two terms, one of them representing the polarization produced by a point source (P_0), and the other a correction for finite size of the source (P_1):

$$P = P_0 + P_1, \quad (3)$$

$$P_0 = -\tfrac{3}{16}\sigma_T \sin^2 i F(e) n_0 \xi, \quad (4)$$

$$F(e) = \frac{3}{e}\left[\frac{1}{3}\frac{3-e^2}{e}\sinh^{-1}\left(\frac{e}{\sqrt{1-e^2}}\right) - 1\right], \quad (5)$$

$$P_1 = \tfrac{3}{8}\sigma_T \sin^2 i n_0 a\psi, \quad (6)$$

with

$$\psi = \sum_{n=0}^{\infty}\frac{(2n-3)!!}{2^n n!}\int_0^1 (1 - 3\mu^2)\exp(\phi)E_{2n}(\phi)d\mu, \quad (7)$$

and

$$\phi = \frac{a}{\xi}(1 - e^2 + e^2\mu^2)^{1/2}; \quad (8)$$

E_{2n} is the $2n$th exponential integral. In what follows we will change n_0 by ρ_0/U, U being the mean molecular weight of the shell's gas.

Equation (3) depends upon five unknown quantities: ρ_0, ξ, a, i, and e, which describe the physical and geometrical properties of the shell, and may be used to study its evolution.

In the previous section, during the interpretation of the intrinsic polarization, the assumption of an envelope which expands without changing its geometry appeared reasonable. Thus, deriving logarithmically equation (3), keeping e and i constant, one obtains:

$$\frac{1}{P}\frac{dP}{dt} = \frac{1}{\rho_0}\frac{d\rho_0}{dt} + \frac{1}{\xi}\frac{d\xi}{dt} + \frac{P_1}{P}\left(1 + \frac{\Theta}{\psi}\right)\left(\frac{1}{a}\frac{da}{dt} - \frac{1}{\xi}\frac{d\xi}{dt}\right), \quad (9)$$

where

$$\Theta = \frac{\xi}{a}\sum_{n=1}^{\infty}\frac{(2n-3)!!}{2^n n!}$$
$$\times \int_0^1 (1 - 3\mu^2)\phi\exp(\phi)[E_{2n}(\phi) - E_{2n-1}(\phi)]d\mu.$$

The photospheric radius, $a(t)$, was obtained from the model
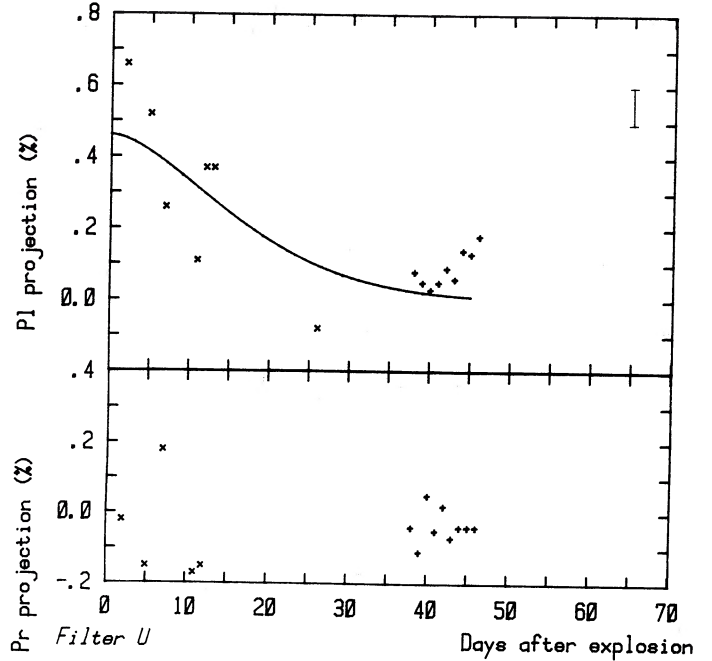
FIG. 2*a*
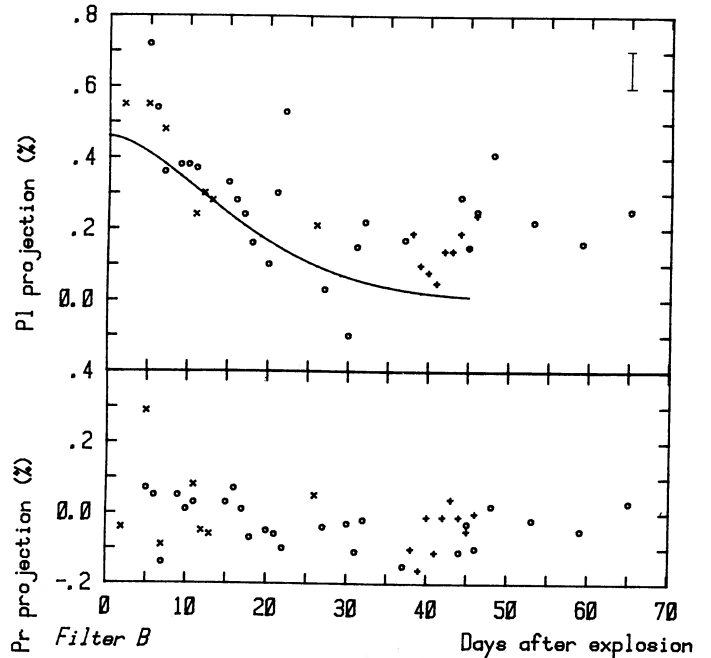
FIG. 2*b*

FIG. 2.—(*a*) Temporal behavior of the parallel and perpendicular projections (Pl and Pr as defined in text) of the intrinsic polarization of SN 1987A in the *U* filter. *Plus*, observations from San Juan. *Cross*, observations from the literature. Solid line superposed on the Pl projection represents the fitting of the expression $Pl(t)/Pl(0) = \exp[-(t/\zeta_p)^j]$ to the observations in all filters until March 30 [Pl(0) = 0.46%, $\zeta_p = 19.6$ days, and $j = 1.63$]. Representative error bar is also indicated. (*b*) Same as (*a*) in the *B* filter, plus the observations from La Plata (indicated by open circle). (*c*) Same as (*b*) in the *V* filter. (*d*) Same as (*b*) in the *R* filter. (*e*) Same as (*b*) in the *I* filter.
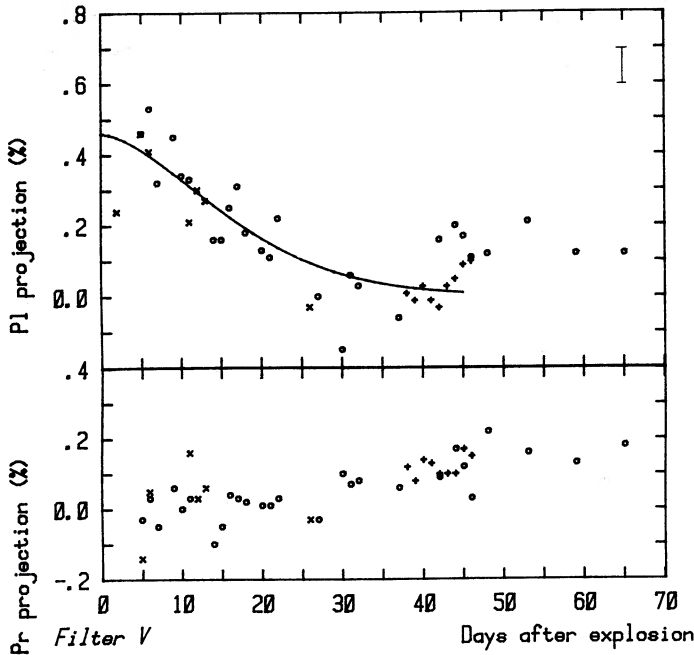
FIG. 2c
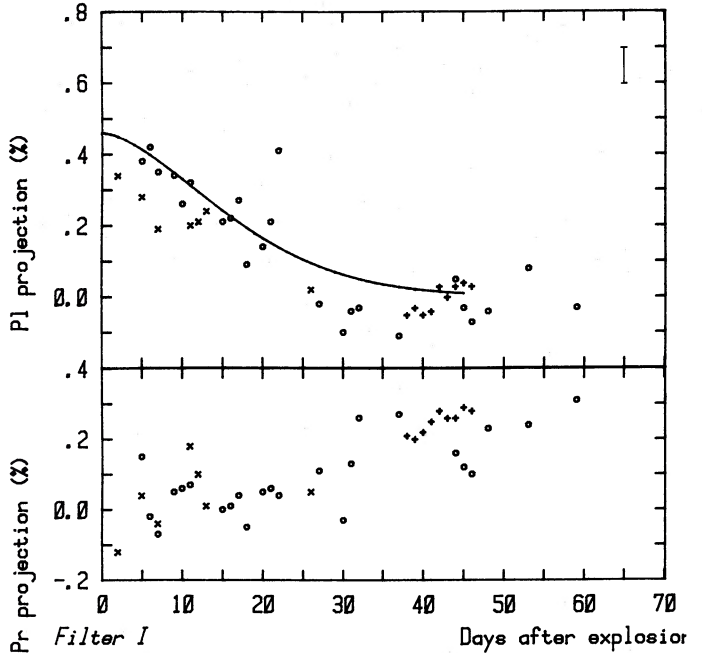
FIG. 2e
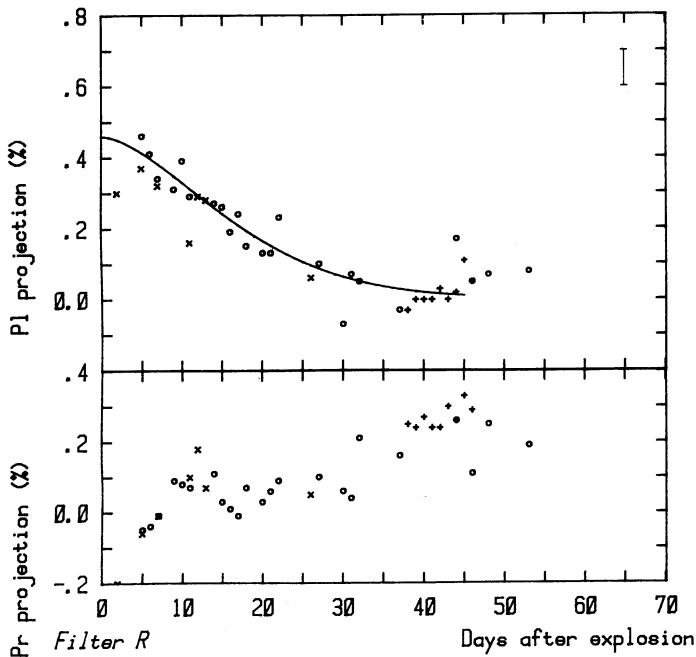
FIG. 2d

computed by Woosley, Pinto, and Ensman (1988) for a 15 $M_\odot$ progenitor.

In order to determine ρ_0 and ξ it is necessary to find another independent relation between them. Since the polarization is produced by the electrons which are being ejected through the photosphere in the envelope, it is necessary to look for an equation which relates the mass-loss rate and the mass of the envelope. The total mass of the envelope can be written as

$$M = \frac{8\pi}{1 - e^2} \rho_0 \xi^3 \left[1 + G(e)\frac{a}{\xi} + H(e)\frac{a^2}{\xi^2} \right], \quad (10)$$

where

$$G(e) = \frac{(1 - e^2)^{1/2}}{e} \tan^{-1} \left[\frac{e}{(1 - e^2)^{1/2}} \right],$$

and

$$H(e) = \frac{1 - e^2}{2e} \sinh^{-1} \left[\frac{e}{(1 - e^2)^{1/2}} \right].$$

If equation (10) is logarithmically derived, the following expression arises:

$$\frac{1}{M}\frac{dM}{dt} = \frac{1}{\rho_0}\frac{d\rho_0}{dt} + \frac{3}{\xi}\frac{d\xi}{dt} + \frac{a}{\xi}\left(\frac{1}{a}\frac{da}{dt} - \frac{1}{\xi}\frac{d\xi}{dt} \right)$$
$$\times \frac{G(e) + 2H(e)(a/\xi)}{1 + G(e)(a/\xi) + H(e)(a/\xi)^2}. \quad (11)$$

Equations (9) and (11) determine the evolution of ρ_0 and ξ if the terms $d \ln (Pl)/dt$ and $d \ln (M)/dt$ are given. The quantity $d \ln (Pl)/dt$ is straightforwardly obtained from Figure 2. We fitted a curve of the form

$$P_l(t) = P_l(t = 0) \exp \left[-\left(\frac{t}{\zeta_p}\right)^j \right] \quad (12)$$

to the first component, and derived the following values for the parameters: Pl(0) = 0.46%, ζ_p = 19.6 days, j = 1.63.

On the other hand,

$$\frac{dM}{dt} = 4\pi\rho_0 a^2 \left[v(t) - \frac{da}{dt} \right], \quad (13)$$

where $v(t)$ is the velocity of the ejected mass which was computed by fitting an equation similar to equation (12) to the radial velocity observations of Hα of Blanco et al. (1987). The values obtained for the parameters were $v(0) = 27.0 \ 10^3$ km s^{-1}, ζ_v = 17.6 days, j = 0.45.

In order to solve equations (9) and (11), the initial value of ρ_0 or ζ (which are related through eq. [3]), and the chemical composition of the shell must be fixed. We used the relation $n = \rho(1 + X)/2H$, and adopted an hydrogen mass abundance $X = 0.7$, which is typical for Population I stars. In addition, the eccentricity and inclination of the shell have to be assumed. We found that with fixed e and i, the behavior of the density after a couple of weeks of evolution was almost independent of the $\rho_0(0)$ choice. Woosley and Weaver (1986) suggested that ~ 20 days after the explosion the photosphere reaches a density in the order of 10^{-13} g cm^{-3}. Since the photospheric density has to decrease, $\rho_0(0)$ must be greater than this value. Thus, we have computed models with $\rho_0(0) = 5 \times 10^{-13}$ g cm^{-3}, $\rho_0(0) = 10^{-12}$ g cm^{-3}, and $\rho_0(0) = 4 \times 10^{-12}$ g cm^{-3}. Since there is no way to fix *a priori* the geometrical factors, e and i, of the shell, they were kept as free parameters in our models. However, if we adopt a value for $\rho_0(0)$, the initial mass of the shell is determined by these geometrical factors, if the observed polarization is to be reproduced. This relation may be used to limit the values of e and i, provided that the initial mass is estimated independently. In Figures 4a and 4b we present level contour plots of the initial mass against i and e for two values of $\rho_0(0)$. According to Blanco *et al.* (1987), the hydrogen mass of the outer layer of SN 1987A is less than $\sim 10^{-2}\, M_\odot$ (a few days after explosion). This value may be used in order to limit the region of the i, e-plane in which realistic models may be located. Models with low values of e and i should be rejected, since they require a large initial mass. On the other hand, models with high values of e and i cannot reproduce the observed amounts of polarization.

After computing some models, an additional restriction was found. With the inclination fixed, small values of e allowed by the initial mass condition lead to unrealistic results (i.e., decreasing typical size and/or decreasing total mass of the shell). In Figures 5a–5c, two models with $\rho_0(0) = 10^{-12}$ g cm^{-3}, two with $\rho_0(0) = 4 \times 10^{-12}$ g cm^{-3}, and one with $\rho_0(0) = 5 \times 10^{-13}$ g cm^{-3} are presented. The characteristic parameters of the models are given in Table 5.

A remarkable feature is that neither a change of the initial photospheric density, nor that of the initial mass of the outer layers results in a substantial change of the typical size of the shell. On day 30 the size of the envelope is $\sim 1.4 \times 10^{15}$ cm, in all cases. As we have mentioned above, we look for models that reach a photospheric density of $\sim 10^{-13}$ g cm^{-3} after ~ 20 days. In this sense, models with $\rho_0(0) = 4 \times 10^{-12}$ g cm^{-3} are the most suitable ones. However, this argument does not allow us to disregard some of the models with lower initial photospheric densities. Finally, and according to this, the total mass of the polarizing shell after 30 days of evolution would be between 0.35 and 1.2 $M_\odot$.
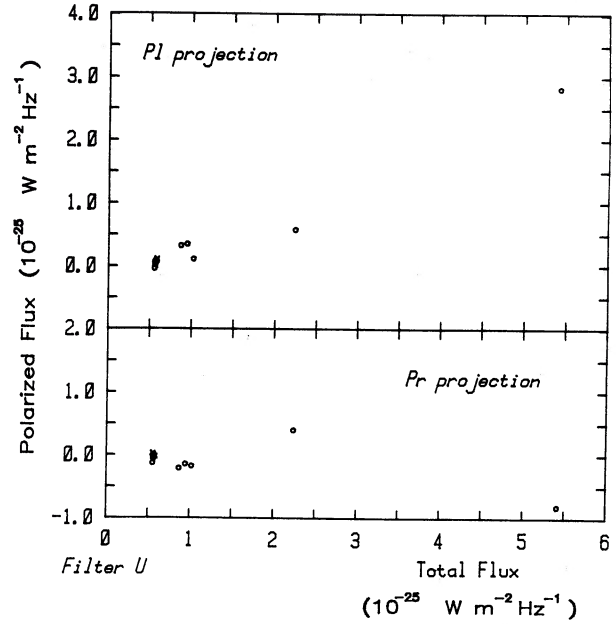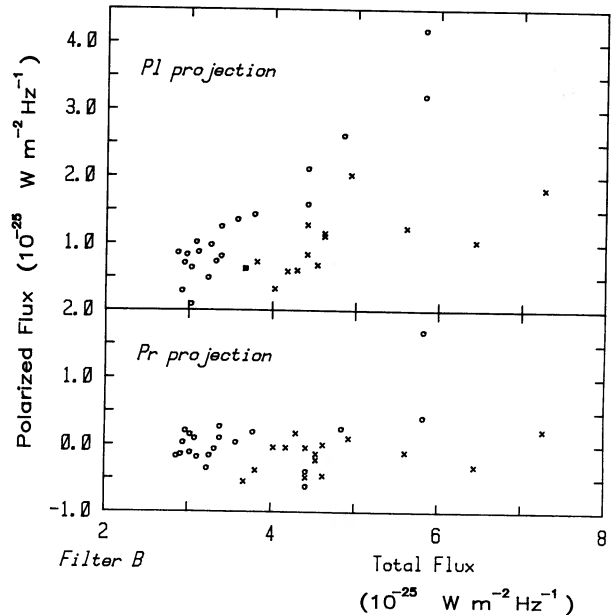

FIG. 3a

FIG. 3b

FIG. 3.—(a) Plots of the polarized flux of each projection vs. the total flux, in the U filter. Circles and crosses represent observations before and after March 30, respectively. (b) Same as (a) for the B filter. (c) Same as (a), for the V filter. (d) Same as (a), for the R filter. (e) Same as (a), for the I filter.

TABLE 5
PARAMETERS OF MODELS

Model	e	i	$\rho_0(0)$	$\zeta(0)$	$M(0)$
1	0.40	20	0.5	0.066	0.006
2	0.40	15	1.0	0.063	0.010
3	0.60	10	1.0	0.039	0.005
4	0.45	7	4.0	0.048	0.024
5	0.55	5	4.0	0.041	0.020

NOTE.—The quantity i is given in degrees; $\rho_0(0)$ is given in units of 10^{-12} g cm^{-3}; $\zeta(0)$ is given in units of 10^{15} cm; $M(0)$ is given in solar masses.

V. CONCLUSIONS

Original *UBVRI* linear polarimetric observations of SN 1987A, obtained between 1987 February 28 and April 29, are presented.

The observed polarization was separated into a foreground component and an intrinsic polarization (IP) of the supernova. The IP initially shows a decreasing trend, which is associated
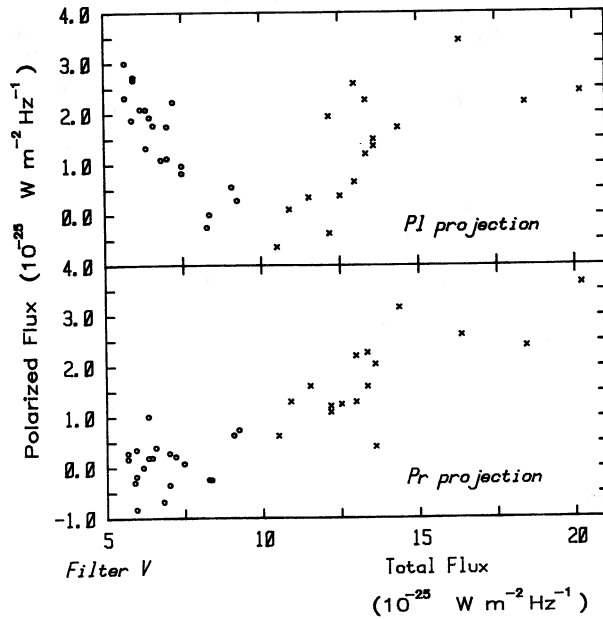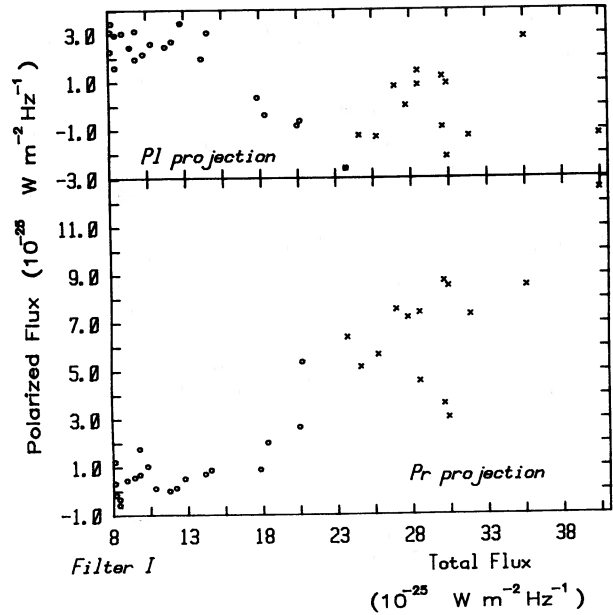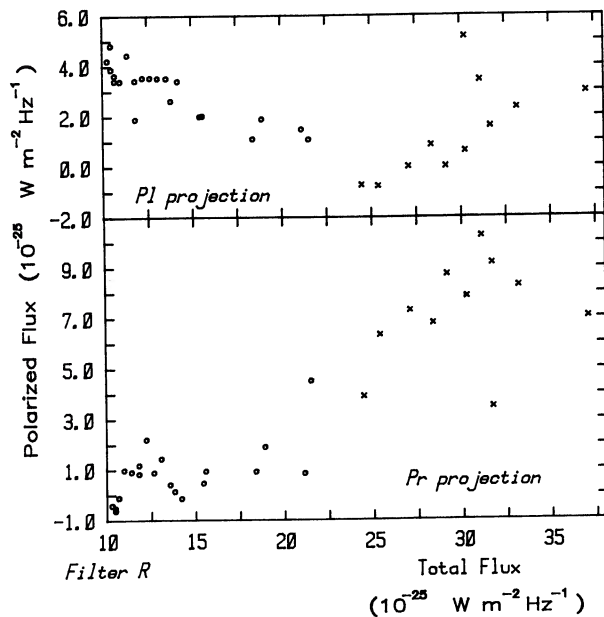
FIG. 3c

FIG. 3e

FIG. 3d

with changes in the polarizing features of the expanding outer shells of the supernova. Also, this initial IP is wavelength independent, suggesting that the scattering opacity is mainly Thomson scattering.

On the additional hypothesis that the outer layers are ellipsoidal, the evolution equations for the photospheric density and typical size of the envelope are derived. Assuming an exponential density profile for the optically thin layers, we solve these equations. This allows us to study the expansion of the external layers during the first few weeks after explosion.

Notably, disregarding the initial parameters adopted, all the models lead to a similar typical size. In all cases, this size results 1.4×10^{15} cm, approximately.

The models are unable to provide information about the inclination and excentricity of the shell separately. However, realistic results are obtained only for a small range of these parameters. The inclination should be lesser than 15°, while the eccentricity should be between 0.40 and 0.60, which implies an axis ratio of the shell between 0.80 and 0.92. It is interesting that Jeffery (1987), using synthetic polarization spectra, has obtained a good fitting for the Balmer lines with values of the axis ratio between 0.60 and 0.80. This confirms the necessity of including a significant amount of asymmetry ($\sim 20\%$) in supernovae explosion models.

After ~ 30 days, the polarization changes both its orientation and wavelength dependence. This suggests that the effect
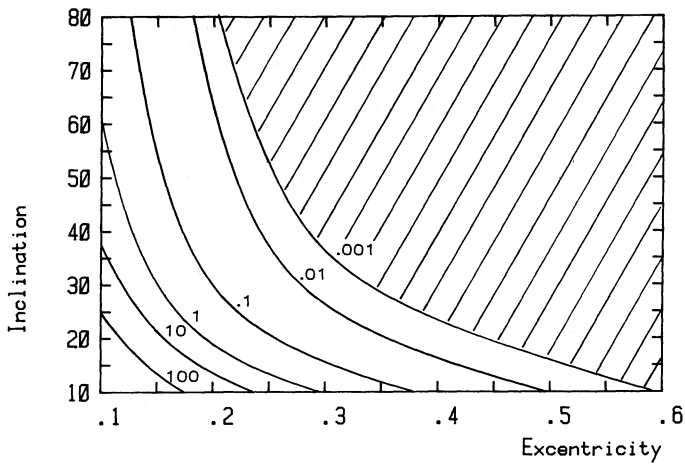
FIG. 4a
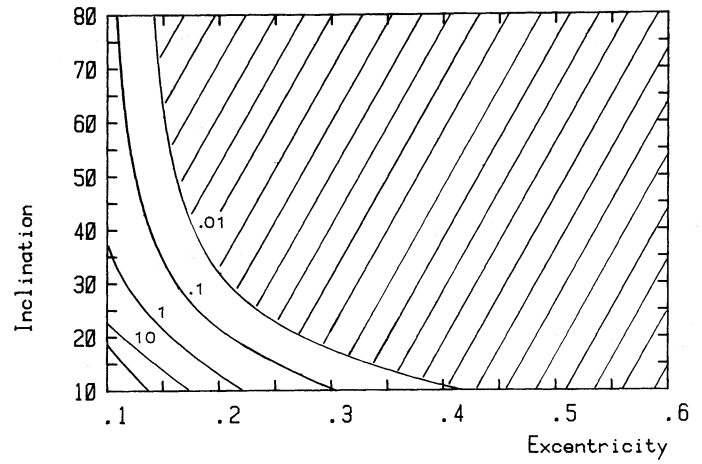
FIG. 4b

FIG. 4.—(a) Level contour plots of the initial mass of the shell required to reproduce the initial polarization. The value of the mass on each contour is indicated at the right of the contour. Units are solar masses. Shaded area indicates a forbidden region for the parameters e and i (see text). The initial density used was 10^{-12} g cm^{-3}. (b) Same as (a), using an initial density of 4×10^{-12} g cm^{-3}.
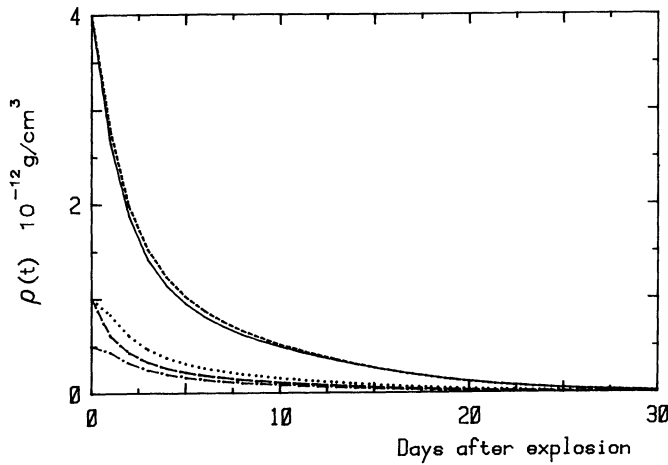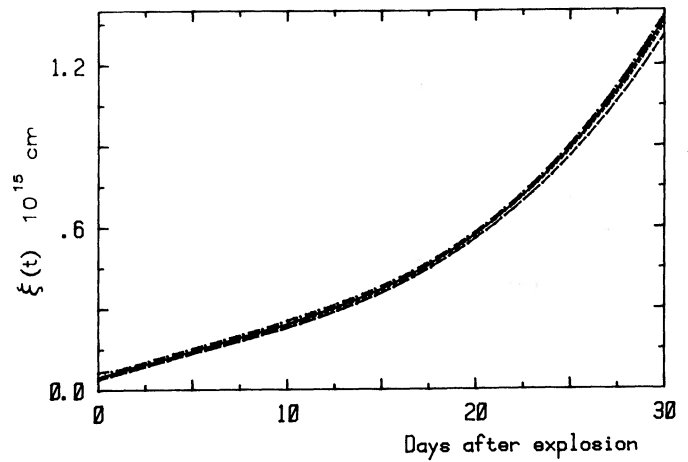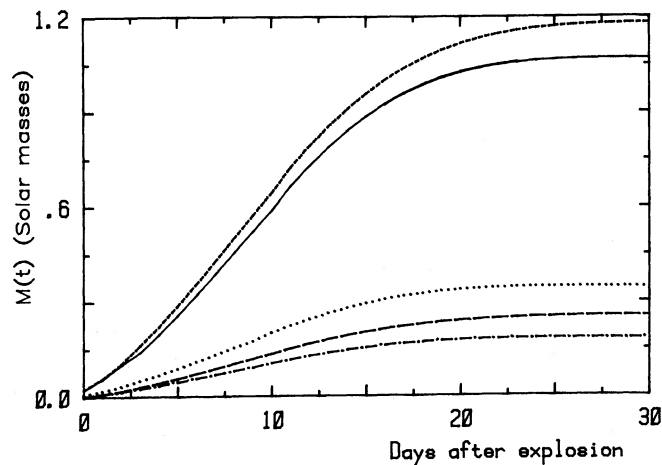

FIG. 5a

FIG. 5b

FIG. 5c

FIG. 5.—(a) Evolution of the density for five of the computed models. *Dotted-dashed line*: model 1. *Dotted line*: model 2. *Long-dashed line*: model 3. *Solid line*: model 4. *Short-dashed line*: model 5. (b) Evolution of the typical size for five of the computed models. Meaning of the different line styles is the same as in (a). (c) Evolution of the mass for five of the computed models. Meaning of the different line styles is the same as in (a).

306

of the absorption on the total opacity becomes important after this time. However, there may be a completely different polarizing mechanism. In particular, the possible relation between this second polarization component and the speckle companion of SN 1987A (Nisenson *et al.* 1987) should be considered.

In a previous paper (Clocchiatti *et al.* 1988), a less elaborated model led us to conclude that the observed IP could have been produced by low amounts of asymmetry. In view of the results of this work, that conclusion should be disregarded.

REFERENCES

Barret, P. 1987a, *IAU Circ.*, No. 4337.
———. 1987b, *IAU Circ.*, No. 4340.
Bailey, J. A., Ogura, K., and Sato, S. 1987, *IAU Circ.*, No. 4351.
Benvenuto, O., Clocchiatti, A., Feinstein, C., García, B., Luna, H., Méndez, M., and Morrell, N. 1987, *IAU Circ.*, No. 4358.
Bessell, M. S. 1979, *Pub. A.S.P.*, **91**, 589.
Blanco, V. M., *et al.* 1987, *Ap. J.*, **320**, 589.
Brown, J. C., and McLean, I. S. 1977, *Astr. Ap.*, **57**, 141.
Cassinelli, J. P., Nordsiek, K. H., and Murison, M. A. 1987, *Ap. J.*, **317**, 290.
Clayton, G. C., Martin, P. G., and Thompson, I. 1983, *Ap. J.*, **265**, 194.
Clocchiatti, A., Méndez, M., Benvenuto, O., Feinstein, C., Marraco, H., García, B., and Morrell, N. 1988, in *Proc. 4th George Mason Workshop on Astrophysics, SN 1987A in LMC*, ed. M. Kafatos and A. Michalitsianos (Cambridge: Cambridge University Press), p. 70.
Cousins, A. W. J. 1976, *M.N.R.A.S.*, **81**, 25.
Cropper, M., and Bailey, J. A. 1987, *IAU Circ.*, No. 4319.
Deeming, T. J. 1968, *Vistas Astr.*, **10**, 125.

Gliese, W. 1969, *Catalogue of Nearby Stars* (Veröff. Astr. Rechen-Instituts, Heidelberg), No. 22.
Hamuy, M., Suntzeff, N., González, R., and Martin, G. 1988, *A.J.*, **95**, 63.
Jeffery, D. J. 1987, *Nature*, **329**, 419.
Magalhaes, A. M., Benedetti, E., and Roland, E. H. 1984, *Pub. A.S.P.*, **96**, 383.
Nisenson, P., Papaliolios, C., Karovska, M., and Noyes, R. 1987, *Ap. J.* (*Letters*), **320**, L15.
Rudy, R. J. 1978, *Pub. A.S.P.*, **90**, 688.
Sanduleak, N. 1970, *Contr. Cerro Tololo Inter-American Obs.*, No. 89.
Schmidt, Th. 1976, *Astr. Ap. Suppl.*, **24**, 357.
Schwarz, H. E. 1987, *IAU Circ.*, No. 4339.
Schwarz, H. E., and Mundt, R. 1987, *Astr. Ap.*, **177**, L4.
Serkowski, K., Mathewson, D. S., and Ford, V. L. 1975, *Ap. J.*, **196**, 261.
Shapiro, P. R., and Sutherland, P. G. 1982, *Ap. J.*, **263**, 902.
Wilking, B. A., Lebofsky, M. J., and Rieke, G. H. 1982, *A.J.*, **87**, 695.
Woosley, S. E., and Weaver, T. A. 1986, *Ann. Rev. Astr. Ap.*, **24**, 205.
Woosley, S. E., Pinto, P. A., and Ensman, L. 1988, *Ap. J.*, **324**, 466.

OMAR BENVENUTO, ALEJANDRO CLOCCHIATTI, CARLOS FEINSTEIN, HUGO MARRACO, and MARIANO MÉNDEZ: Observatorio Astronómico, Paseo del Bosque s/n, 1900 La Plata, Argentina